Combined Deep Learning with Multiview Modeling for Robust 3D Wound Segmentation Using Mobile Phone Images⋆

Rania Niri[a,*], Evelyn Gutierrez[b], Hassan Douzi[a], Yves Lucas[c], Sylvie Treuillet[c], Benjamin Castaneda[b] and Iván Hernandez[d]

[a]*IRF-SIC Laboratory, Ibn Zohr University, Agadir, Morocco*
[b]*Department of Engineering, Pontifical Catholic University, Lima, Peru*
[c]*PRISME Laboratory, Orleans University, Orleans, France*

ARTICLE INFO

ABSTRACT

Accurate chronic wound segmentation and precise area measurements are critical components to ensure a successful management of chronic wounds in photography-based wound analysis. Various deep learning methods based on fully convolutional neural networks have performed successfully wound area segmentation. Unfortunately, the performance of these 2D methods from single view can greatly be affected by body curvature and perspective viewing. Moreover, 2D methods do not provide depth information which may be useful for a more accurate assessment. Hence the need for a robust 3D reconstruction tool to overcome these drawbacks. Thus, 3D wound assessment devices have limited accessibility and expensive. On the other hand, 3D reconstruction from multiple views using a simple smartphone became an attractive option for researchers. By combining 2D segmentation results of each view, we can obtain the segmentation in the 3D model. However, DL suffer from poor segmentation precision due to angle and distance variation in the Multiview sequence especially for small size wounds. Thus, inaccurate segmentation can lead to improper diagnosis and inaccurate wound management. In this work, we proposed a novel method to improve DL segmentation in all the views regardless of camera shooting angle and distance using the 3D model and best view selection. Further, several experiments were carried out to select effectively the best view. The proposed method outperformed DL results on a test dataset of 270 images of diabetic foot ulcers. DICE index and IoU score regarding wound class were improved from 36.53% and 29.48% to 86.33% and 77.09% respectively to achieve an overall DICE and IoU scores of 93.04% and 86.61% including background class. In addition, MAE and RMSE decreased from 0.164 and 0.036 to attain 0.004 and 0.019 respectively. The experimental results show the robustness of our method to perform precise segmentation regardless of wound size, position and viewing angles and distance and demonstrate the potential of our method to perform accurate 3D wound segmentation.

1. Introduction

Chronic wounds are a major health issue that affect population quality of life and lead to a huge burden for the healthcare systems worldwide [10]. Chronic wounds are injuries which take more than 12 weeks to heal [25] and they include venous ulcers, pressure injuries, diabetic ulcers, traumatic and surgical ulcers, etc. These wounds are complex and heal gradually depending on their severity. Wound healing process is a complicated procedure that requires regular check-ups by wound specialists. The fundamentals of a successful clinical care require fast decision making and clinicians with considerable knowledge and technical skills. Tracking wound size including length, width, depth, and circumference is a key indicator for preventing healing and evaluating response to treatment.

There are various methods to inspect the healing progress, most commonly, practitioners use rudimentary modalities such as rulers, wound outline tracing, and wound filling [20] [19] [3]. These manual methods are often harmful, time con-suming and require wound contact which can carry high risk of infection. In addition, the accuracy of these techniques relies on the subjective diagnosis of the clinician depending on his expertise and personal experience. However, for a relevant wound assessment, it is vital that the ideal measuring tool must be unbiased, accurate and consistent since the diagnosis largely depends on the used measurement method.

Over the last years, the application of photography became increasingly popular in clinical practice with the increase in computational power. It avoids direct wound contact and enable clinicians to achieve more consistent and accurate wound assessment. Digital photography considerably reduced delays in care decisions. More recently, Smartphone wound image analysis have been extensively used to assist clinicians in qualitative diagnosis. Smartphones are low-cost, noninvasive, user-friendly and are already equipped with high-resolution cameras. The rapid rise of smartphone's camera resolution got a lot of clinician's interest about capturing high-quality images during wound examination.

Segmentation is an essential step in photography-based wound analysis because it influences the outcome of the entire assessment process. Most of research works have focused on 2D image segmentation. Although, the promising results of prior works in literature, there are many limitations. First, 2D methods can be greatly affected by body

*Corresponding author

✉ rania.niri@edu.uiz.ac.ma (R. Niri)
ORCID(s):

Figure 1: Sample images from our heterogeneous chronic wounds database

curvature. Second, perspective distortion can yield to different segmentation results. Third, a single view does not provide depth information that is essential to perform an accurate chronic wound monitoring.

3D imaging techniques overcomes the shortcomings and limitations of 2D methods. 3D imaging technique have been introduced to improve assessment in different medical areas [17]. Existing 3D scanning devices are actually expensive and not adapted to the clinical practice which requires a portable and simple to use tool [1] [11] [2]. Alternatively, two or more converging pairs of views can be used to construct the 3D surface area of the wound using a simple smartphone camera. The constructed 3D model can be monitored from any angle and perspectives. In addition, the obtained 3D point clouds can offer much more detailed information about the lesion regardless of the wound position and size. However, automatic three-dimensional segmentation remains a considerable challenge because it requires 3D labels which are time-intensive and difficult to obtain. To avoid the need of 3D training data, 3D image segmentation will be obtained from the 2D segmentation of each image slice using scene fusion. The results of 2D segmentation using DL are merged and directly mapped on the mesh surface of the 3D model.

Though, DL suffer from poor segmentation precision due to high angle and distance variation in the Multiview sequence. To produce a correct segmentation the image has to be taken perpendicularly to the wound surface what we call frontal view. In addition, the wound should be located in the center of the image and with a distance not to close not far from the camera. If the angle or the distance from the wound slightly changed from a view to another one, the accuracy can quickly decrease especially for large or highly curved lesions. Moreover, for small size wounds, DL failed completely to segment the non-frontal views. However, it is important to include different viewing perspectives of the wound in the 3D model to obtain a robust 3D representation of it. Thus, inaccurate 2D segmentation can influence the final 3D results. To this end, we propose a novel Deep Learning based wound segmentation method that overcomes large angles and distance variation using best view selection and 3D model reconstruction. The method goes through several steps: (1) semantic segmentation of the 2D image sequence (2) 3D model reconstruction and best view selection (3) reprojection of best view segmentation on each image slice to get the final segmentation on the 3D model.

We demonstrated the effectiveness of our method by conducting comprehensive experiments. In this work, we focused our experiments on diabetic foot ulcers as these wounds tend to be smaller than other types of chronic wounds and more complex to segment. Similarly, diabetic foot ulcers combine wound characteristics, ischemia and infection [18]. The majority of diabetic ulcers are located in the lower extremities and often result in lower limb amputation. Even when properly managed, these wounds may take more than expected amount of time to heal [28]. Our method provides more precise and robust segmentation from any angle and distance. At the same time, it avoids 3D-CNNs complexity and 3D data costs. Moreover, our methodology is applicable to all wound types from the largest to the smallest ones regardless of their location and healing stage. Furthermore, the proposed system could allow clinicians to have a precise measurement tool that assist in developing more responsive treatment plan for patients with chronic wounds and that could be also used as effective telemedicine tool.

2. Literature Review

2.1. Wound Segmentation

Most of published researches focused on wound assessment by measuring physical dimension (perimeter, surface, volume and depth). Wound segmentation was performed using two main approaches: machine learning and deep learning. Prior to the rise of deep learning in medical imaging, wound detection methods mostly utilized machine learning models [35] [31] [34]. These models generally use classifiers such as SVM which have the advantage of not being very data intensive. However, they require hand-crafted features to extract color and texture descriptors. Moreover, they suffer from a poor generalization in uncontrolled lighting environments. These problems were resolved by using deep learning networks (DNN). Recent research works have focused on DNN to address wound segmentation task using convolutional neural networks (CNN) or fully convolutional networks (FCN). To deal with the massive training data requirement in DL, many researchers used data augmentation and transfer learning [39]. Also, other researchers adopted hybrid methods combining neural networks and ML classifiers.

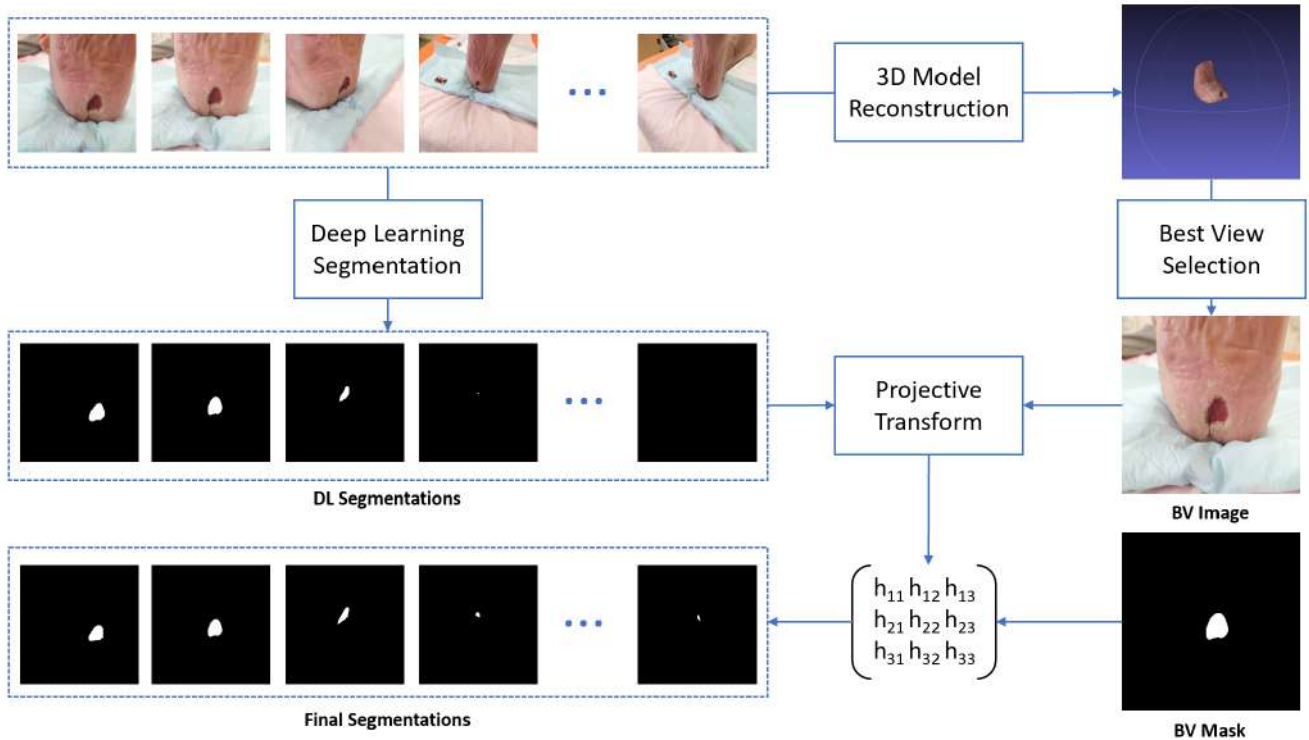Alzubaidi et al. [5] developed a novel deep convolu-

Figure 2: Workflow of the proposed 3D segmentation method based on DL and BV selection

tional neural network named DFU_QUTNet for diabetic foot skin classification (normal and abnormal skin). Features extracted by DFU_QUTNet were used to train SVM and KNN classifiers. While Goyal et al. [14], trained a Faster R-CNN with Inception V2 using two-tier learning with the MS COCO dataset. Their objective was to detect DFU localization using a relatively small dataset of DFU images. A post-processing step was required to improve the results. In a recent work [32], they performed foot ulcer segmentation using a lightweight convolutional framework based on MobileNetV2 and connected component labelling using a dataset consisting of 1109 foot ulcer images. Newer methods with EfficientDet [30] provided superior ulcer detection accuracy during MICCAI conference challenge using DFUC 2020 dataset [8]. This dataset consists of 4500 diabetic foot ulcer images with expert annotations. Although the proposed methods were highly accurate in wound localization [13] [38], both studies did not address wound segmentation precision and wound area measurement. Despite the outstanding performance of DL methods, they also have some downsides though. Mainly this technique fail in case of important viewing angle and distance variation or when the object to segment is too small.

3D reconstruction is commonly used to improve the performance of a 2D segmentation method. It helps to enhance wound detection from various angles and distances independently of their size and shape. Many researches have addressed 3D wound segmentation using traditional computer vision methods [36] [12] [21]. Very few works have performed automated 3D medical images segmentation using deep neural networks. Kamnitsas et al. [16] presented a

3D CNN architecture with fully connected CRF for automatic brain lesion segmentation that outperformed the state-of-the-art techniques. Similarly, Dolz et al. [9] used a 3D and fully convolutional neural network for the sub-cortical brain structure segmentation using MRI scans. In [33], the authors have extended U-net to 3D U-Net to realize three-dimensional semantic segmentation of Intervertebral Disc. The downside of using DL for 3D medical imaging is their computational and memory requirements in addition to network size and complexity.

In order to address all the above limitations, we proposed a novel deep learning framework which achieves 2D to 3D semantic segmentation making use of the best view selection. In the next section, we will describe and discuss the implementation and development of our proposed method.

2.2. 3D model creation

Given the disadvantages of traditional wound assessment, technology that uses imaging to perform non-contact measurements began to increase in popularity in the 1990s. In particular, measurements involving 3D information of the wound are useful, as more accurate and precise information can be obtained than with the use of 2D imaging.[37, 6, 40, 15, 22]

To create 3D models, two types of methodologies are distinguished: active and passive methods. In the active approach, a signal is sent to the object of interest and the reflection of this signal is used to obtain the depth at each part of the object. Then, using numerical methods, the 3D point cloud can be inferred. This methodology is accurate
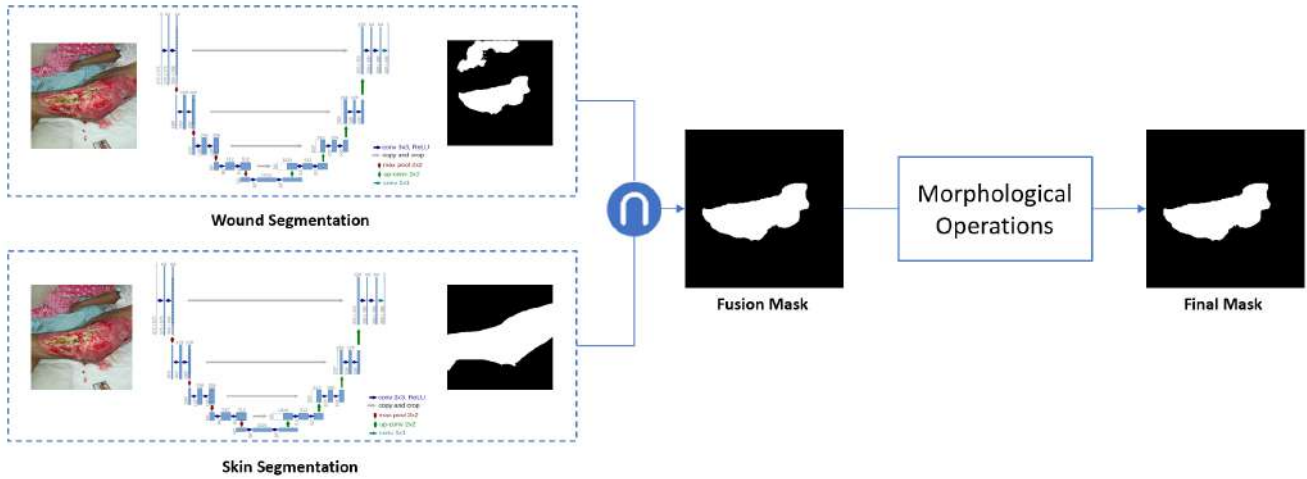
Figure 3: 2D chronic wounds segmentation pipeline

and fast; however, the equipment needed is often expensive, not portable and requires some training to use.

Passive methods, on the other hand, are methods in which no signal interferes with the object. They only require a sensor that passively obtains images from the radiation naturally emitted by the object. Some passive 3D reconstruction techniques are stereo vision and structure from motion, which only require images from digital cameras to obtain the 3D point cloud.

In particular, structure from motion (SfM) is a very attractive technique as it has very few requirements: a single camera obtaining images from different viewpoints with overlapping information between the images. Additionally, implementations of SfM are found in several free software packages, making this technique accessible to a wide audience.

In particular, SfM can be used for wound assessment. Previous studies have demonstrated the potential of its usefulness. In [40], volume calculations using 3D models created with SfM pipeline are studied and it is evidenced that the volume calculations approximate those obtained with a high-precision laser scanner. In [7], the potential of using SfM for wound monitoring is shown again, it is proven that it allows using a simple data acquisition protocol with portable devices to obtain models with results similar to those of an industrial laser scanner.

Moreover, recent studies show the potential of other algorithms for passive reconstruction can be fully implemented with the smartphone CPU and GPU. In [24] and [23], they show the potential of their algorithms in the reconstruction of various objects, the latter using an algorithm close to SfM. However, their use in the medical context remains to be evaluated.

3. Methodology

Our contribution can be summarized as follows (See Figure. 2) :

(1) We proposed a robust wound segmentation method with an effective background removal using DL.

(2) We performed 3D model reconstruction using a simple acquisition protocol with a monocular camera from a low-cost smartphone and using SfM to infer the 3D structure.

(3) We proposed a novel pipeline from 2D to 3D DL based wound segmentation that overcomes large angles and distance variation using camera view selection and 3D model reconstruction.

(4) Finally, we demonstrated the efficiency and effectiveness of our method by conducting experiments and analyses on various diabetic foot ulcers that tend to be smaller and harder to segment than other types of chronic wounds.

3.1. DL segmentation

We built a large annotated chronic wound database consisting of 569 images covering all pathologies such us diabetic foot ulcers, burns, pressure injuries, etc. Mostly captured from a relatively perpendicular angle (See Figure. 1). This dataset contains various wounds with distinct size and in different healing stages. The images were taken in several medical sites with different cameras and without any strict protocol regarding lighting conditions. Consequently, the segmentation task was quite challenging. Most images have different backgrounds including lots of regions similar to the wound bed which may threaten the segmentation. However, segmenting chronic wounds demands a high level of accuracy, small marginal segmentation errors can lead to wrong measurements and poor user experience in clinical settings. To this end, we proposed a robust wound segmentation method comprising wound delineation and skin correction for an effective background removal without increasing the complexity of deep neural networks.

To perform wound delineation, we based our segmentation on our previous work [26] while proposing more robust background elimination using skin correction. We opted for the state-of-the-art semantic segmentation network U-net for

medical images [27]. U-net has proven to be very powerful specifically in the field of biomedical images segmentation using very little data.

Our method consists of two main stages (See Figure. 3). First, wound area extraction which aim to eliminate all background elements. Second, the obtained wound segmentation mask will be post-processed by skin detection algorithm. Its goal is to remove all non-skin pixels from background. Thus, only segmented elements inside skin area will be conserved. When skin segmentation map combined with the wound map, we are able to provide more accurate segmentation. Finally, the generated mask is further refined by hole filling and the removal of missing small points in the segmentation map using morphological operations (i.e., erosion, dilation, opening and closing) [29]. The performance of the proposed segmentation procedure helped to improve the accuracy to reach a Jaccard index of 98.48% and a Dice score of 99.26% instead of 94.96% and 97.25% in the previous version [26] using the same testing set. The proposed 2D segmentation method overcomes perfectly complex background elimination and uncontrolled lighting conditions, but it still can be greatly affected by camera angle and high distance variation especially for small wounds such as diabetic foot ulcers.

3.2. 3D modeling

Given the advantages in terms of required devices and portability, we selected SfM for passive 3D reconstruction to be used for 3D model creation in this study.

The 3D modeling pipeline starts with a SIFT feature extraction and matching after which the structure-from-motion algorithm is used to infer the 3D structure. A sparse point cloud is created that serves as the basis for the 3D model. Next, the Semi-Global Matching (SGM) algorithm is used to create depth maps in order to create a dense 3D point cloud and surface where the texture is superimposed. As a final step, a Laplacian filter is applied to reduce noise that may appear during the reconstruction of the dense 3D model.

The described process for creating the 3D mesh is performed using an open source software: Alicevision[4] which is possible to run automatically through Python. Figure. 4 shows the pipeline based on SfM for the 3D mesh creation.
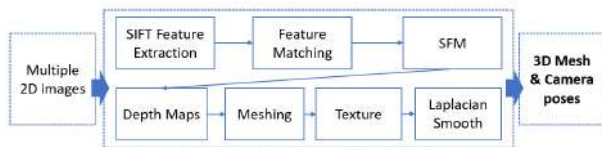

Figure 4: 3D model creation pipeline

As a result of this process, we obtain a dense 3D mesh for each wound and estimation of the camera poses for the reconstruction. The camera poses are useful later to transfer the 2D segmentation to the 3D model and vice-versa.

Figure 5: Sample of Best view Selection

3.3. 3D Wound Segmentation

Since each DL segmentation mask can produce a different outline of the wound in the 3D model, the distance and angle between the wound surface and the camera is used to select the most appropriate view. The distances and angles are calculated as follows:

1. The 3D model is projected onto the camera plane and using the corresponding DL segmentation mask, the temporal segmentation of the wound is created in the 3D model.

2. From the point cloud corresponding to the wound surface, the Euclidean distance between each point and the center of the camera is calculated.

3. For each triangle on the wound surface, the angle between the principal camera ray and the normal of each triangle is calculated.

4. Finally, we use the median of the distances and the median of the angles calculated above to summarize the relative position of each camera with respect to the wound.

Four strategies are used to select the most appropriate camera view. For this, the relative position of each camera to the wound calculated above is used:

- Strategy 1: The view with the most acute camera-to-wound angle is selected.

- Strategy 2: The view with the closest camera-to-wound distance is selected.

- Strategy 3: The view with the closest distance within the 5 images with the sharpest camera-to-wound angles is selected.

- Strategy 4: The view with the most acute angle among the 5 images with the closest distances between camera and wound.

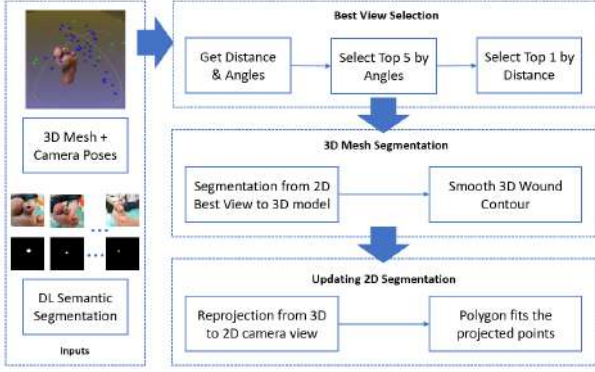In Figure. 5, the selection of a view with the strategy 3 is shown as an example.

Figure 6: Workflow of the 3D model re-projection to update semantic segmentation

3.4. Updating 2D semantic segmentation

After selecting an appropriate view with one of the 4 strategies, the corresponding segmentation mask is used to create the final segmentation of the wound in the 3D model. This segmentation is combined with a post-processing of the 3D mesh to smooth the wound edges which consists of subdividing the wound contour in the 3D mesh and using a simple neighbor averaging based on a wound indicator to obtain a smoothed wound contour.

Finally, the 3D wound segmentation resulting from the above process is projected onto the corresponding views of all 2D images. The result is a collection of updated 2D segmentation masks. Figure 6 shows the complete process performed to create the 3D mesh segmentation and update the semantic segmentation on the 2D images with the proposed methodology.

4. Experimental Results

4.1. Dataset and Material

In cooperation with Dr. Villeneuve in the diabetology service of the CHRO (Regional Hospital of Orleans in France), we collected a data set of 270 diabetic foot images taken from 7 subjects during multiple clinical visits. The used system included a Xiaomi Note7 and an add-on temperature sensor FlirOne. The acquisition protocol includes several points of views with different viewing angles and distances for each wound.

For creating the 2D images that serve as the ground truth, the segmentation was annotated directly on the 3D model manually and using MeshLab then reviewed by wound care experts. The segmented 3D model is then projected onto each of the camera views and the corresponding wound segmentation masks are obtained for each single view.

4.2. Metrics

To evaluate the segmentation performance, two metrics were adopted:

- The Dice Similarity Coefficient (DICE) : Quantifies the overlap between the obtained segmentation mask and the ground truth. This metric is popularly used by researchers in the medical image segmentation field.

$$DICE = \frac{2TP}{2TP + FP + FN} \qquad (1)$$

where TP is true positive, FP is false positive, TN is true negative, and FN is false negative.

- The Intersection Over Union (IoU) : Is one of the most commonly used metrics in semantic segmentation that determines the accuracy of the segmented mask against the ground truth.

$$IoU = \frac{TP}{TP + FP + FN} \qquad (2)$$

where TP is true positive, FP is false positive, TN is true negative, and FN is false negative.

- Root Mean Square Error (RMSE) : RMSE was used to measure the difference per pixel between the reference image and the obtained mask. The smaller the value of RMSE, the better the segmentation performance.

$$RMSE(X,Y) = \sqrt{\frac{\sum_{i=1}^{n}(X_i - Y_i)^2}{n}} \qquad (3)$$

Where X and Y are the ground truth and the segmented mask, n is the total number of pixels in the image.

- Mean Absolute Error (MAE) : Finally, segmentation mask and the ground truth mask were compared using the mean absolute error

$$MAE(X,Y) = \frac{\sum_{i=1}^{n}|X_i - Y_i|}{n} \qquad (4)$$

Where X and Y are the ground truth and the segmented mask, n is the total number of pixels in the image.

4.3. Analysis and Discussion

To investigate the performance of the proposed 3D method over 2D, we compared the segmentation results achieved by our 2D segmentation scheme including robust background elimination using Deep Learning (DL) against those obtained by including the 3D model with best view segmentation reprojection (BV+DL). In the following experiments, we consider the four different strategies introduced in (Section 3.3) to choose effectively the best view for the proposed method.

Dice and IoU were evaluated on DFU dataset across different angles and distances. Since the ulcer area in test images is much smaller than the background, these two metrics were measured locally to focus only on the segmented area. The plots in Figure. 7) demonstrate that among all different angles and distances, the 2D method based on DL
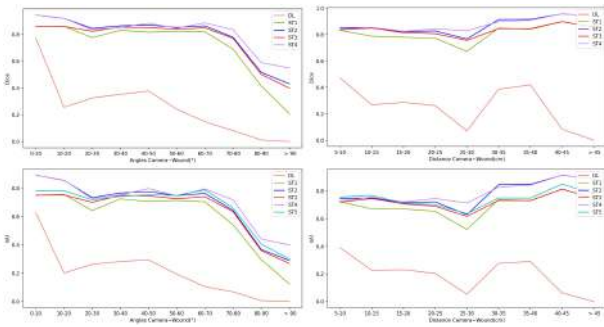
Figure 7: Dice and IoU performance on the test set across different angles and distances
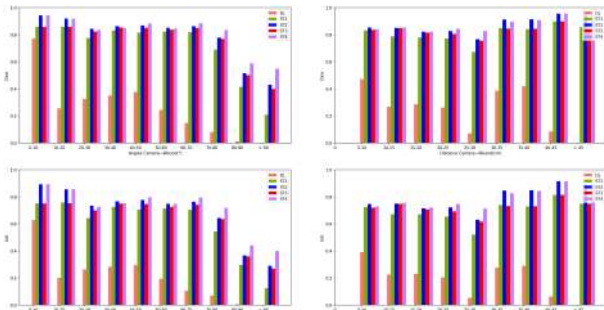

Figure 8: Dice and IoU barplots on the test set across different angles and distances

Table 1
Area calculation (px)

	Area Calculation (px)					
Patient	Real_area	DL	ST1	ST2	ST3	ST4
Pat 1	514	385	**456**	**456**	**456**	**456**
Pat 2	4912	1629	**4835**	4194	3813	3813
Pat 3	59	11	**59**	**59**	58	57
Pat 4	94	8	91	91	91	**94**
Pat 5	359	293	**341**	**341**	**341**	**341**
Pat 6	51	0	29	**51**	**51**	42
Pat 7	324	227	297	**316**	297	**316**

DL. However, despite the high segmentation accuracy using the BV reprojection, the segmentation performance drop significantly once rotation angle exceeds 80° for all proposed strategies.

Further analysis of the 3D cloud plots of DL compared with the 3D based methods in terms of segmentation accuracy measured by DICE score with their corresponding 2D representation are shown in Figure. 9. Each test image is represented by a point in the 3D cloud. Blue color corresponds to low segmentation accuracy, while orange corresponds to high segmentation precision. We observe that the proposed method improves the accuracy as well as the stability of segmentation. The 2D plots illustrate the very good performance of ST1, ST2, ST3 and ST4 in predicting the wound area across all angles and distance values compared to DL.

Another interesting experiment to explore the effectiveness of the proposed strategies over DL method, is to quantify the number of detected pixels in the predicted segment. The results of wound area calculation (AC) in comparison with the real area (RA) corresponding to the ground truth for each patient were reported in Table. 1. Overall, ST1, ST2, ST3 and ST4 produce high AC scores close to the RA of the ground truth according all patients and consistently outperforms DL scores. The four strategies performed similarly but, in most of the cases, ST2 was the closest to the ground truth.

For further analysis, Figure. 10 and Figure. 11 illustrate the distribution of mean absolute error (MAE) and root mean square error (RMSE) respectively, between the ground truth mask and the obtained segmentation mask of each of the tested methods. Low values of MAE and RMSE correspond to high segmentation performance. The box-plots of DL method indicate larger MAE and RMSE resulting in lower segmentation quality. On the contrary, all BV+DL strategies show lower MAE and RMSE compared to DL. This correlates with higher segmentation accuracy. Moreover, we observe that ST2 attains the lowest MAE and RMSE in comparison to other strategies. These results corroborate our previous findings about ST2 performing better than ST1, ST3 and ST4 as it offers the highest performance with lowest segmentation error. This shows that ST2 has not only better accuracy, but also better robustness.
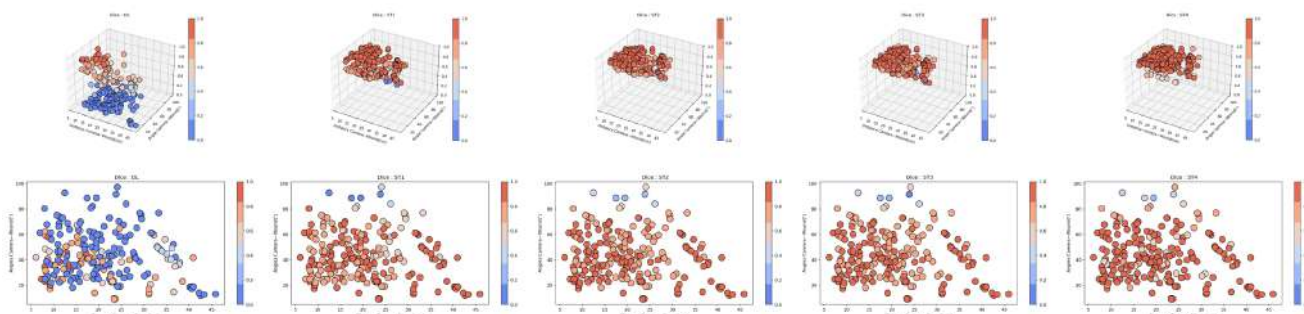
Qualitative comparison of both methods DL and ST2

only shows the worst segmentation performance according to DICE and IoU values compared to the proposed strategies.

As illustrated in Figure. 8, DL method can be greatly affected by viewing angle and distance. Starting with angle variation, to obtain a good segmentation, the angle should be as perpendicular as possible to the wound bed, so closer to 0°. Bigger angle variation can result in lower segmentation accuracy. The best results were achieved for an angle variation less than 10°, what we call frontal views. Then DL performance started decreasing gradually the largest the angle value became. For an angle value over 80° DICE and IoU were of 0%. Thus, DL method totally failed to detect the wound area in those images. Moreover, DL is rather sensitive to distance variation upper to 10 centimeters. The best segmentation was performed with a distance value between 5 and 10 cm. Otherwise, the method failed completely to segment the wound especially when the distance exceeds 40 cm.

However, reprojecting the segmentation from the BV using the 3D model helped to improve the two metrics across all angles and distance values regarding all proposed strategies. The performance metrics of the obtained segmentation are much higher than DL. In addition, the results show high segmentation consistency among all points of view for the four strategies. Furthermore, ST2 and ST4 consistently outperforms other strategies. These two methods reached the highest performance in term of Dice and IoU for the largest angles and furthest distances. Meanwhile, the metrics using ST1 were lower than the other strategies but still better than

Figure 9: Comparison of the 3D point cloud of DL against the four proposed strategies using Dice score

Figure 10: Box-plot of Mean Absolute Error
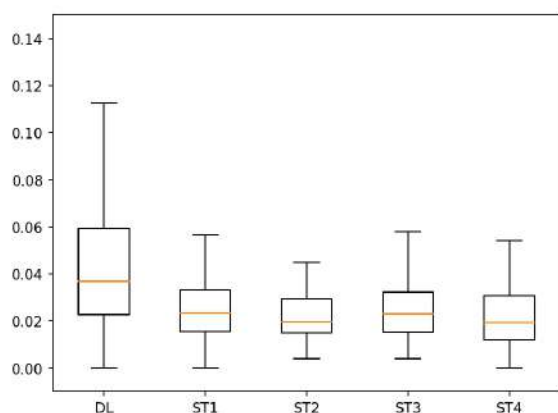

Figure 11: Box-plot of Root Mean Square Error

Table 2
A Summary of segmentation improvement

	Dice	IoU	MAE	RMSE
DL	36.53%	29.48%	0.164	0.036
ST1	83.49%	73.56%	0.054	0.023
ST2	**86.33%**	**77.09%**	**0.004**	**0.019**
ST3	84.52%	74.21%	0.012	0.023
ST4	85.40%	76.00%	0.020	0.020

our method robustness.

Segmentation results on the 3D model are shown on Figure. 13. These results are obtained by the fusion of single views segmentations. To do this, first we performed wound segmentation on each image of the multiview sequence, then these results are merged and directly mapped on the mesh surface of the 3D model.

Comparing quantitative and qualitative results of the 2D method based on single view DL segmentation and the proposed method based on 3D model reconstruction and best view segmentation reprojection, we can see a huge improvement on metrics and segmentation quality. By comparing different strategies to select effectively the best view, we found out that ST2 performed the best and achieved the highest performance. This strategy consists on selecting the view with the best distance. Reprojecting the BV segmentation widely improved both Dice and IoU scores and decreased segmentation error on test dataset (See Table. 2). The proposed method not only overcomes the limitations of DL due to wound size and location, but also guarantees a precise segmentation among different shooting angles and distances. Therefore, our method has a great potential to be used in clinical practice for an effective 3D assessment of chronic wounds using a simple smartphone.

5. Conclusion

In this paper, we presented a novel Deep Learning based method for 3D semantic segmentation of chronic wounds that overcomes the limitations of 2D methods. A smartphone is used as an alternative way to capture the wound from multiple views which is cost-effective, user-friendly and did not require any strict protocol during acquisitions.
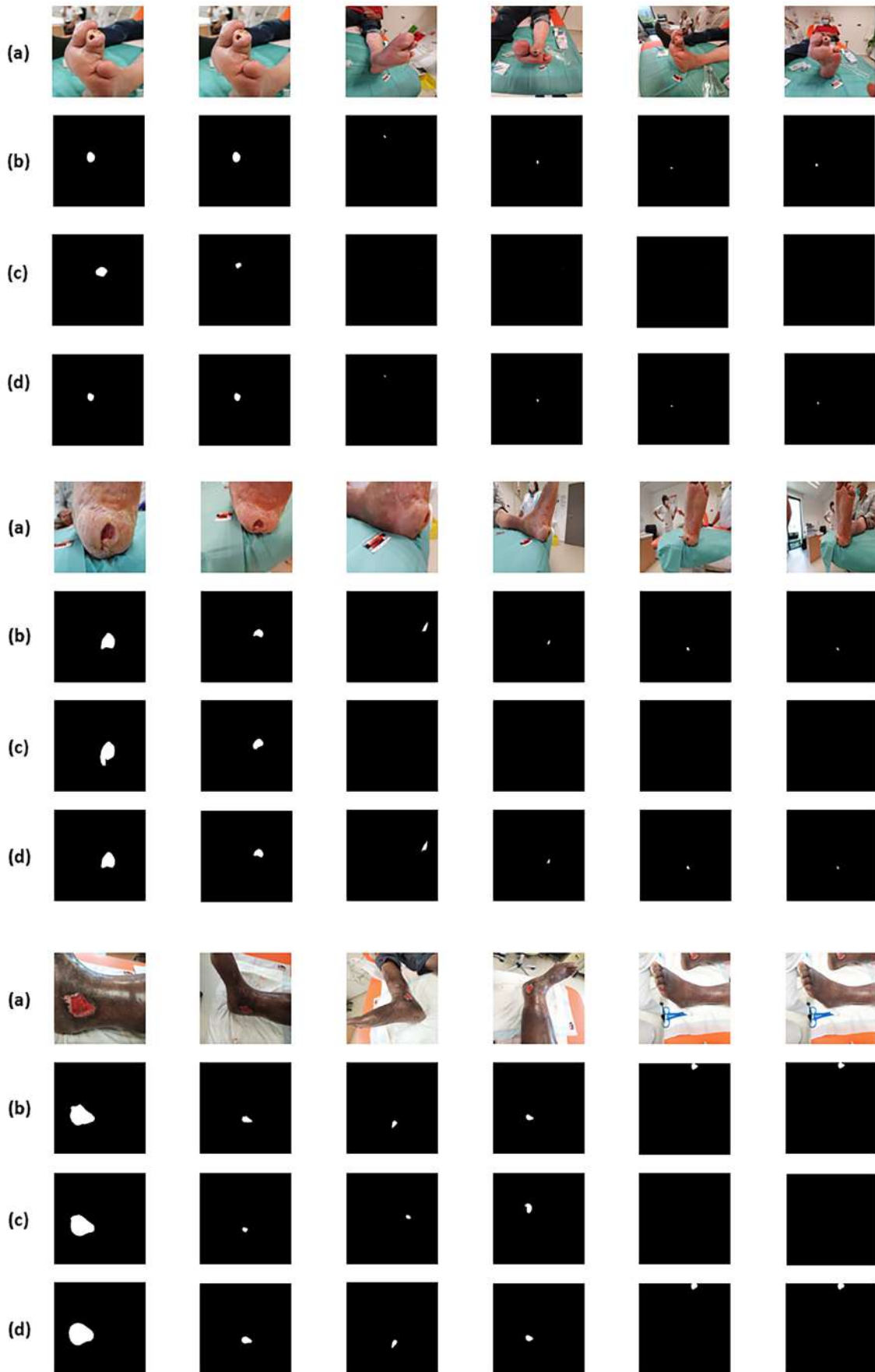
against the ground truth are shown in Figure 12. We chose image sequences of three patients with different DFU size (small, medium and big) to visually represent our results. The segmentation results achieved by the proposed method performs better to segment the ulcer. It successfully detected the wound area of different sizes and shapes regardless of the acquisition angle or distance. The segmentation is much more accurate. In addition, the correct detection of the wound in case of deep learning failures is a statement of

Figure 12: Segmentation results: (a) original images, (b) Ground truth, (c) output of DL method and (d) output of our method

We attempted to solve weak segmentation accuracy problem due to big angle and distance variation during the Multiview wound acquisition. Our approach first improves DL segmentation using the 3D model and best view selection. The result is a robust segmentation in all the views regardless of camera shooting angle and distance. The obtained 2D segmentation masks are then merged and mapped into the 3D model to generate the final segmentation of the wound in 3D. Comprehensive experiments have demonstrated the robustness of our method in comparison with single view DL segmentation. Further, experiments were carried out to identify the best strategy for the BV selection. In addition, the results show that ST2 based on best distance selection achieved the highest accuracy and lowest error rates. Segmentation performance has been widely improved for all metrics compared to DL. Consequently, 3D wound segmentation is more precise. Such a system can be used in clinical settings for all kinds of chronic wounds regardless of their size, shape and location. Furthermore, it is harmless and avoids the risk of infection. A future research would be to extend our method to perform wound tissue classification task. More accurate and complete assessment could be established. Moreover, we plan to use the proposed method as an effective weakly supervised data augmentation approach to deal with the lake of annotated datasets in medical field.
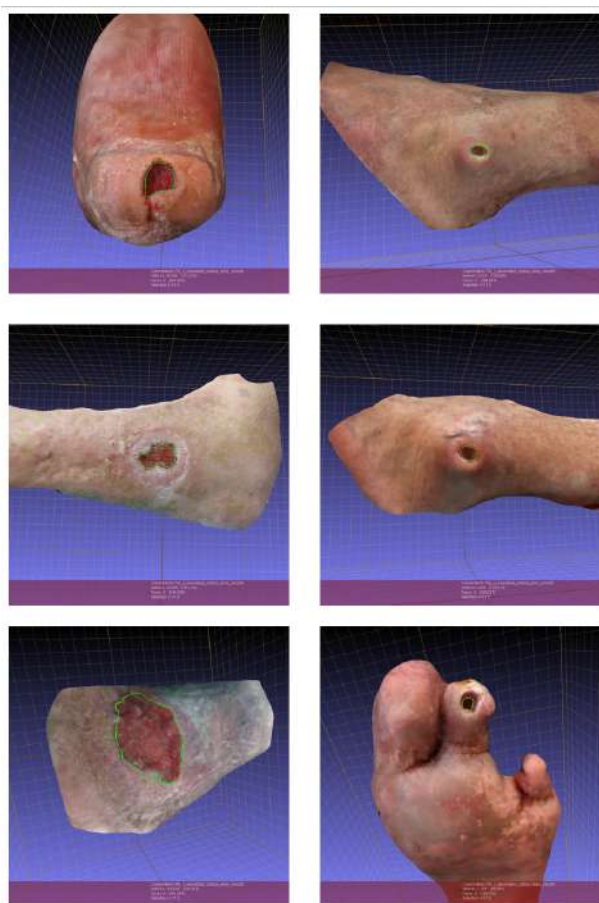

Figure 13: Segmentation results on the 3D model

References

[1] , 2018. Aranzmedical silhouette. https://www.aranzmedical.com/.

[2] , 2018. Woundworks insight. https://woundworks.com/.

[3] Ahn, C., et al., 2008. Advances in wound photography and assessment methods. Advances in skin & wound care 21, 85–93.

[4] AliceVision, 2018. Meshroom: A 3D reconstruction software. URL: https://github.com/alicevision/meshroom.

[5] Alzubaidi, L., Fadhel, M.A., Oleiwi, S.R., Al-Shamma, O., Zhang, J., 2020. Dfu_qutnet: diabetic foot ulcer classification using novel deep convolutional neural network. Multimedia Tools and Applications 79, 15655–15677.

[6] Bowling, F.L., King, L., Fadavi, H., Paterson, J.A., Preece, K., Daniel, R.W., Matthews, D.J., Boulton, A.J.M., 2009. An assessment of the accuracy and usability of a novel optical wound measurement system. Diabetic Medicine 26, 93–96. URL: http://doi.wiley.com/10.1111/j.1464-5491.2008.02611.x, doi:10.1111/j.1464-5491.2008.02611.x.

[7] Casas, L., Treuillet, S., Valencia, B., Llanos, A., Castañeda, B., 2015. Low-cost uncalibrated video-based tool for tridimensional reconstruction oriented to assessment of chronic wounds, Cartagena de Indias, Colombia. p. 928711. URL: http://proceedings.spiedigitallibrary.org/proceeding.aspx?doi=10.1117/12.2070999, doi:10.1117/12.2070999.

[8] Cassidy, B., Reeves, N.D., Joseph, P., Gillespie, D., O'Shea, C., Rajbhandari, S., Maiya, A.G., Frank, E., Boulton, A., Armstrong, D., et al., 2020. Dfuc2020: Analysis towards diabetic foot ulcer detection. arXiv preprint arXiv:2004.11853 .

[9] Dolz, J., Desrosiers, C., Ayed, I.B., 2018. 3d fully convolutional networks for subcortical segmentation in mri: A large-scale study. NeuroImage 170, 456–470.

[10] Fife, C.E., Eckert, K.A., Carter, M.J., 2018. Publicly reported wound healing rates: the fantasy and the reality. Advances in wound care 7, 77–94.

[11] Filko, D., Cupec, R., Nyarko, E.K., 2016. Detection, reconstruction and segmentation of chronic wounds using kinect v2 sensor. Procedia Computer Science 90, 151–156.

[12] Filko, D., Cupec, R., Nyarko, E.K., 2018. Wound measurement by rgb-d camera. Machine Vision and Applications 29, 633–654.

[13] Goyal, M., Hassanpour, S., 2020. A refined deep learning architecture for diabetic foot ulcers detection. arXiv preprint arXiv:2007.07922 .

[14] Goyal, M., Reeves, N.D., Rajbhandari, S., Yap, M.H., 2018. Robust methods for real-time diabetic foot ulcer detection and localization on mobile devices. IEEE journal of biomedical and health informatics 23, 1730–1741.

[15] Jørgensen, L.B., Halekoh, U., Jemec, G.B., Sørensen, J.A., Yderstræde, K.B., 2020. Monitoring Wound Healing of Diabetic Foot Ulcers Using Two-Dimensional and Three-Dimensional Wound Measurement Techniques: A Prospective Cohort Study. Advances in Wound Care 9, 553–563. URL: https://www.liebertpub.com/doi/10.1089/wound.2019.1000, doi:10.1089/wound.2019.1000.

[16] Kamnitsas, K., Ledig, C., Newcombe, V.F., Simpson, J.P., Kane, A.D., Menon, D.K., Rueckert, D., Glocker, B., 2017. Efficient multi-scale 3d cnn with fully connected crf for accurate brain lesion segmentation. Medical image analysis 36, 61–78.

[17] Karatas, O.H., Toy, E., 2014. Three-dimensional imaging techniques: A literature review. European journal of dentistry 8, 132.

[18] Keast, D.H., Bowering, C.K., Evans, A.W., Mackean, G.L., Burrows, C., D'Souza, L., 2004. Contents: Measure: A proposed assessment framework for developing best practice recommendations for wound assessment. Wound Repair and Regeneration 12, s1–s17.

[19] Langemo, D., Anderson, J., Hanson, D., Hunter, S., Thompson, P., 2008. Measuring wound length, width, and area: which technique? Advances in skin & wound care 21, 42–45.

[20] Little, C., McDonald, J., Jenkins, M., McCarron, P., 2009. An overview of techniques used to measure wound area and volume. Journal of wound care 18, 250–253.

[21] Liu, C., Fan, X., Guo, Z., Mo, Z., Eric, I., Chang, C., Xu, Y., 2019. Wound area measurement with 3d transformation and smartphone images. BMC bioinformatics 20, 1–21.

[22] Malone, M., Schwarzer, S., Walsh, A., Xuan, W., Al Gannass, A., Dickson, H.G., Bowling, F.L., 2020. Monitoring wound progression to healing in diabetic foot ulcers using three-dimensional wound imaging. Journal of Diabetes and its Complications 34, 107471. URL: https://linkinghub.elsevier.com/retrieve/pii/S1056872719310050, doi:10.1016/j.jdiacomp.2019.107471.

[23] Muratov, O., Slynko, Y., Chernov, V., Lyubimtseva, M., Shamsuarov, A., Bucha, V., 2016. 3DCapture: 3D Reconstruction for a Smartphone, in: 2016 IEEE Conference on Computer Vision and Pattern Recognition Workshops (CVPRW), IEEE, Las Vegas, NV, USA. pp. 893–900. URL: http://ieeexplore.ieee.org/document/7789606/, doi:10.1109/CVPRW.2016.116.

[24] Ondruska, P., Kohli, P., Izadi, S., 2015. MobileFusion: Real-Time Volumetric Surface Reconstruction and Dense Tracking on Mobile Phones. IEEE Trans. Visual. Comput. Graphics 21, 1251–1258. URL: https://ieeexplore.ieee.org/document/7165662/, doi:10.1109/TVCG.2015.2459902.

[25] Patel, S., Srivastava, S., Singh, M.R., Singh, D., 2019. Mechanistic insight into diabetic wounds: Pathogenesis, molecular targets and treatment strategies to pace wound healing. Biomedicine & Pharmacotherapy 112, 108615.

[26] Rania, N., Douzi, H., Yves, L., Sylvie, T., 2020. Semantic segmentation of diabetic foot ulcer images: Dealing with small dataset in dl approaches, in: El Moataz, A., Mammass, D., Mansouri, A., Nouboud, F. (Eds.), Image and Signal Processing, Springer International Publishing, Cham. pp. 162–169.

[27] Ronneberger, O., Fischer, P., Brox, T., 2015. U-net: Convolutional networks for biomedical image segmentation, in: International Conference on Medical image computing and computer-assisted intervention, Springer. pp. 234–241.

[28] Sheehan, P., Jones, P., Caselli, A., Giurini, J.M., Veves, A., 2003. Percent change in wound area of diabetic foot ulcers over a 4-week period is a robust predictor of complete healing in a 12-week prospective trial. Diabetes care 26, 1879–1882.

[29] Sreedhar, K., Panlal, B., 2012. Enhancement of images using morphological transformation. arXiv preprint arXiv:1203.2514 .

[30] Tan, M., Pang, R., Le, Q.V., 2020. Efficientdet: Scalable and efficient object detection, in: Proceedings of the IEEE/CVF conference on computer vision and pattern recognition, pp. 10781–10790.

[31] Veredas, F.J., Luque-Baena, R.M., Martín-Santos, F.J., Morilla-Herrera, J.C., Morente, L., 2015. Wound image evaluation with machine learning. Neurocomputing 164, 112–122.

[32] Wang, C., Anisuzzaman, D., Williamson, V., Dhar, M.K., Rostami, B., Niezgoda, J., Gopalakrishnan, S., Yu, Z., 2020. Fully automatic wound segmentation with deep convolutional neural networks. Scientific Reports 10, 1–9.

[33] Wang, C., Guo, Y., Chen, W., Yu, Z., 2019. Fully automatic intervertebral disc segmentation using multimodal 3d u-net, in: 2019 IEEE 43rd Annual Computer Software and Applications Conference (COMPSAC), IEEE. pp. 730–739.

[34] Wang, L., Pedersen, P.C., Agu, E., Strong, D.M., Tulu, B., 2016. Area determination of diabetic foot ulcer images using a cascaded two-stage svm-based classification. IEEE Transactions on Biomedical Engineering 64, 2098–2109.

[35] Wannous, H., Lucas, Y., Treuillet, S., 2008a. Efficient svm classifier based on color and texture region features for wound tissue images, in: Medical Imaging 2008: Computer-Aided Diagnosis, International Society for Optics and Photonics. p. 69152T.

[36] Wannous, H., Lucas, Y., Treuillet, S., 2010. Enhanced assessment of the wound-healing process by accurate multiview tissue classification. IEEE transactions on Medical Imaging 30, 315–326.

[37] Wannous, H., Lucas, Y., Treuillet, S., Albouy, B., 2008b. A complete 3D wound assessment tool for accurate tissue classification and measurement, in: 2008 15th IEEE International Conference on Image Processing, IEEE, San Diego, CA. pp. 2928–2931. URL: http://ieeexplore.ieee.org/document/4712408/, doi:10.1109/ICIP.2008.4712408.

[38] Yap, M.H., Hachiuma, R., Alavi, A., Brungel, R., Goyal, M., Zhu, H., Cassidy, B., Ruckert, J., Olshansky, M., Huang, X., et al., 2020. Deep learning in diabetic foot ulcers detection: A comprehensive evaluation. arXiv preprint arXiv:2010.03341 .

[39] Yu, Y., Lin, H., Meng, J., Wei, X., Guo, H., Zhao, Z., 2017. Deep transfer learning for modality classification of medical images. Information 8, 91.

[40] Zenteno, O., Gonzalez, E., Treuillet, S., Valencia, B.M., Castaneda, B., Llanos-Cuentas, A., Lucas, Y., . Volumetric monitoring of Leishmaniasis ulcers: Can camera be as accurate as laser scanner for treatment monitoring? , 13doi:10.1080/21681163.2018.1546623.